JOURNAL OF SOLID STATE CHEMISTRY 33, 361–369 (1980)

Lattice Dynamics and Hyperfine Interactions of the Intercalation Compounds Fe_xTiS_2 ($x = \frac{1}{4}, \frac{1}{3}$, and $\frac{1}{2}$) and $Fe_{1/3}NbS_2$ from ^{57}Fe Mössbauer Spectroscopy

MOTOMI KATADA* AND ROLFE H. HERBER†

Department of Chemistry, Rutgers University, New Brunswick, New Jersey 08903

Received June 7, 1979; in revised form October 19, 1979

The intercalates Fe_xTiS_2 ($x = \frac{1}{4}, \frac{1}{3}$, and $\frac{1}{2}$) and $Fe_{1/3}NbS_2$ have been prepared and characterized by ^{57}Fe Mössbauer effect spectroscopy. From isomer shift systematics it is inferred that the electron configuration of the iron atom in these compounds is formally +2, high spin. $Fe_{1/2}TiS_2$ shows magnetic ordering at temperatures below about 140 K, and the internal field at 4.2 K is approximately 30 kOe. Temperature-dependent Mössbauer measurements permit a calculation of the effective vibrating mass of the resonant moiety and a lattice temperature as probed by the Mössbauer atom. The former is nearly constant and that expected for a "bare" iron atom, while the latter varies over a significant range for the four title compounds, despite the similarity in the nearest-neighbor environment around the metal atom in all cases. This variation can be accounted for by the differences in the sulfur bonding modes in these compounds.

In view of their potential use in high-temperature stable electrochemical systems, there has recently been a great deal of interest in the electric, magnetic, and crystallographic properties of the first transition metal series intercalates of the dichalcogenides, TiS_2, NbS_2, and TaS_2 (*1–7*). It is expected that extra metal atoms, M, can be inserted into the octahedral interstices between the sulfur layers of TiS_2 because this sulfide has the CdI_2-type layer structure (space group $P\bar{3}m_1$). Indeed, the existence of intercalation compounds such as Fe_xTiS_2 with a NiAs-like type structure has recently been reported by two groups of workers (*8, 9*). Among these intercalates, $Fe_{1/2}TiS_2$ ($FeTi_2S_4$) has been well characterized and a number of studies of the magnetic and crystallographic properties of this system have been reported (*10–14*). For the cases where the intercalation compounds contain one or more appropriate atoms, Mössbauer spectroscopy can be used to elucidate the details of the chemical bonding as well as the lattice dynamics of the metal atom in these compounds. A number of intercalation compounds have been studied (*15–19*) by using Mössbauer effect techniques. In particular, Fatseas *et al.* (*20*) have studied the system $Fe_{1+x}Ti_{2(1+x)}S_4$ ($x = 0$, 0.030, and 0.052) by Mössbauer spectroscopy and reported that the stoichiometric sample ($x = 0$) showed only one iron site with a small magnetic hyperfine inter-

* Present address: Department of Chemistry, Faculty of Science, Tokyo Metropolitan University, Steagaya-ku, Tokyo, Japan.

† To whom correspondence should be addressed.

0022-4596/80/090361-09$02.00/0

action below 155 ± 5 K. Above this temperature only a paramagnetic doublet is observed in the Mössbauer spectra.

In the present investigation, ^{57}Fe Mössbauer studies have been undertaken for the title intercalation compounds over the temperature range $4.2 \leq T \leq 320$ K, in order to examine the systematics of the hyperfine and lattice dynamical parameters for a number of structurally related solids of this type.

Experimental

The compounds Fe_xTiS_2 ($x = \frac{1}{4}, \frac{1}{3}$, and $\frac{1}{2}$) were prepared by heating a stoichiometric mixture of pure Fe metal powder and TiS_2 in evacuated Vycor tubes. After heating to 900°C for 2 days, the mixture was cooled to room temperature, ground, and again maintained (evacuated tube) at 900°C for 1 week. The products were then cooled slowly to room temperature. The TiS_2 used was prepared from Ti sponge and recrystallized sulfur as described earlier (*21*). The sample of $Fe_{1/3}NbS_2$ was prepared by heating the stoichiometric amount of the high-purity elements in an evacuated Vycor tube. The thermal procedure was the same as in the case of Fe_xTiS_2.

X-Ray powder diffraction (CuKα radiation) and chemical analysis confirmed that the obtained products were stoichiometric and single phase.

Temperature-dependent Mössbauer effect measurements were carried out using the constant acceleration spectrometer described in a previous study (*22*). Temperature control was sufficient to ensure stability to better than ±0.5 K for the time interval necessary to accumulate the Mössbauer data at each temperature point. Data reduction was effected using the least-squares matrix inversion program employed in the earlier studies (*22*). The Mössbauer spectrometer was calibrated using NBS SRM 0.85-mil metallic iron foil and the same ^{57}Co-in-palladium source was utilized in collecting all of the data. All isomer shift data are reported with respect to the midpoint of the α-Fe spectrum at 295 ± 2 K. In the thermal study of $Fe_{1/2}TiS_2$, Al powder was used in order to increase the thermal conductivity of the sample (120 mg of $Fe_{1/2}TiS_2$ and 5 mg of Al powder, mixed with silicon grease), and to reduce the thermal gradient across the experimental material.

Results and Discussion

The Mössbauer spectra obtained at 300 K are shown in Fig. 1 for the system Fe_xTiS_2 ($x = \frac{1}{4}, \frac{1}{3}$, and $\frac{1}{2}$) and $Fe_{1/3}NbS_2$. In Fig. 1b, the spectrum of $Fe_{1/3}TiS_2$ shows only a single resonance maximum but the linewidth (full width at half-maximum) suggests the presence of an unresolved quadrupole hyperfine interaction. Except for $Fe_{1/2}TiS$ none of the spectra showed the presence of a magnetic hyperfine interaction over the temperature range $78 \leq T \leq 320$ K. These results are in good agreement with the magnetic data (*8–14*) previously reported

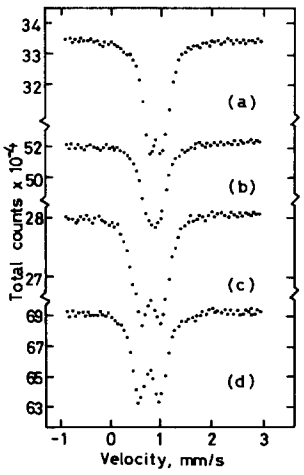

FIG. 1. Mössbauer spectra of the intercalation compounds at 300 K. (a) $Fe_{1/4}TiS_2$, (b) $Fe_{1/3}TiS_2$, (c) $Fe_{1/2}TiS_2$, and (d) $Fe_{1/3}NbS_2$.

TABLE I

SUMMARY OF MÖSSBAUER DATA FOR Fe_xTiS_2 ($x = \frac{1}{4}, \frac{1}{3}$, AND $\frac{1}{2}$ AND $Fe_{1/3}NbS_2$[a]

	IS (mm sec^{-1})[b]			QS (mm sec^{-1})			
	78 K	300 K	$-dIS/dT$[c] (mm sec^{-1} K^{-1})	78 K	300 K	$-d \ln[A(T)/A(78)]/dT$[d] (K^{-1})	Temperature range (K)
$Fe_{1/4}TiS_2$	0.86	0.73	6.69×10^{-4}	0.29	0.30	1.25×10^{-3}	78–320
$Fe_{1/3}TiS_2$	0.90	0.76	6.25×10^{-4}	—	—	0.68×10^{-3}	78–320
$Fe_{1/2}TiS_2$	0.91[e]	0.79	7.26×10^{-4}	0.56[e]	0.44	1.30×10^{-3}[f]	150–320
			5.90×10^{-4}			0.76×10^{-3}	78–200
$Fe_{1/3}NbS_2$	0.92	0.79	6.58×10^{-4}	0.50	0.43	1.04×10^{-3}	200–320

[a] The uncertainties in the IS and QS parameters are approximately ±0.01 mm sec^{-1}.

[b] With respect to α-Fe at 300 K, ±0.01 mm sec^{-1}.

[c] The correlation coefficients for a linear regression are better than 0.994 for all of the compounds discussed. The errors in these temperature dependencies are estimated as $\pm 6.0 \times 10^{-5}$ mm sec^{-1} K^{-1}.

[d] Estimated error, $\pm 5 \times 10^{-5}$ K^{-1}.

[e] At 150 K.

[f] Normalized to 150 K.

for these compounds. The Mössbauer parameters are summarized in Table I.

Isomer Shift

The values of the isomer shift of the iron atom observed in these compounds lie in the range 0.7–1.0 mm sec^{-1} which is normally assigned to high-spin Fe^{2+}, but are smaller than those of halogen containing high-spin ferrous compounds, such as $FeCl_2$ and FeF_2 which lie in the range 1.0 to 1.5 mm/sec with respect to metallic iron. The observed values are similar to those reported for other sulfides in which the Fe atom is located in an octahedral environment. From the Mössbauer data, it may be inferred that the Fe atoms are inserted into the octahedral interstices between the sulfur layers of TiS_2 and NbS_2, respectively, and are formally in the high-spin state. Fatseas *et al.* (*20*) suggested that an isomer shift calibration for the valence state must be used very carefully for $FeTi_2S_4$, since this compound has a metallic-type conductivity which has been attributed to direct cation–cation interactions. It has been reported that the resistivities of these intercalates are typically in the metallic range ($\sim 10^{-4}$ Ω · cm) and that the high electron transport properties can be associated with the partial filling of the titanium or niobium *d* band. In all cases except for $Fe_{1/2}TiS_2$, the Fe–Fe bonding distance is too large for a direct metal atom interaction and thus it is assumed that the Fe ion has only localized *d* electrons. Therefore, the small isomer shift compared with those of other Fe^{2+} compounds may be primarily due to covalent Fe–S bond formation, in consonance with the general rule that isomer shifts of the ^{57}Fe resonance increase with increasing ionicity.

Takahashi and Yamada (*8*) concluded from their magnetic susceptibility data that the Fe atom in $Fe_{1/4}TiS_2$ is trivalent. The present Mössbauer results, however, do not confirm this proposed valency, as can be seen from the isomer shift data summarized in Table 1. The present results are in good agreement with those of Fatseas *et al.* (*20*), who reported an isomer shift for $Fe_{1/4}TiS_2$ of 0.79 mm sec^{-1} at 300 K. In the case of $Fe_{1/3}NbS_2$, Beal and Liang (*26*) assigned a valence state of mixed +2 and +3 to the Fe ions from their optical work. However, as already noted the Mössbauer

data suggest that a more probable assignment is that the iron atom is formally +2, high spin, and the following discussion will be based on this assignment. Magnetic results (*2, 4, 5, 7*) which have been reported also confirm this viewpoint.

Magnetic Ordering

The magnetic properties of $Fe_{1/2}TiS_2$ ($FeTi_2S_4$) have been studied in considerable detail by numerous workers (*8, 14, 15*) due to the apparently anomalous behavior below the magnetic ordering temperature. Although there is general agreement regarding the paramagnetic (Curie–Weiss law) behavior above 140 K deduced from susceptibility versus temperature data, the interpretation of the magnetic behavior below T_N has been the subject of some controversy. The conflicting results have been summarized in detail by Fatseas *et al.* (*20*). The temperature dependence of the Mössbauer resonance of $Fe_{1/2}TiS_2$ is shown in Fig. 2, in which the low resolution of the individual components of the hyperfine spectrum is clearly noticeable. The magnetic ordering temperature estimated from the spectra is about 140 K in agreement with the susceptibility data. The Mössbauer spectra below this temperature are consistent with those reported by Fatseas *et al.* (*20*), who inferred a value of 150 ± 5 K as the magnetic ordering temperature. The internal magnetic field at 4.2 K can be estimated from the total width of the Mössbauer resonance curve, although it has not been possible to resolve the individual components of the magnetic hyperfine spectrum. The value extracted from the liquid helium temperature data is 30 ± 5 kOe, a value which is considerably smaller than those reported for related intercalated chalcogenides such as $Fe_{1/2}VS$ (120 kOe at 4.2 K) and $FeCr_2Se_4$ (89 kOe at 78 K) (*28*). This small observed internal field may be due to the anisotropy of the magnetic field with opposite field contributions. Further investigations (e.g.,

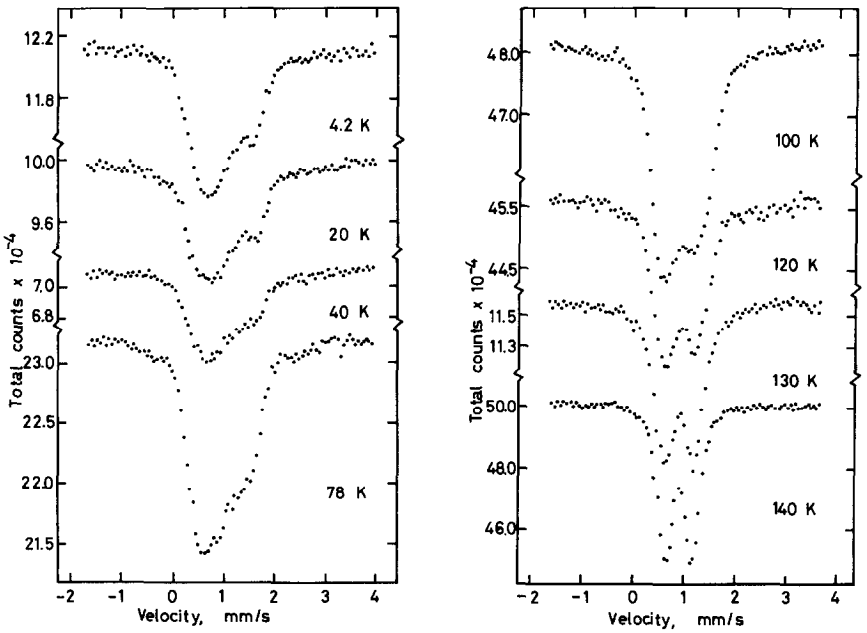

FIG. 2. Mössbauer spectra of $Fe_{1/2}TiS_2$ at eight temperatures in the temperature range $4.2 \leq T \leq 140$ K.

single-crystal experiments) will be required to explore this interpretation in detail.

The Mössbauer spectra of $Fe_{1/4}TiS_2$ at low temperatures ($4.2 \leq T \leq 50$ K) are shown in Fig. 3. The value for the magnetic ordering temperature is not well defined from these data due to broadening of the resonance absorption over a temperature range, possibly due to a magnetic relaxation process occurring in this material. Oka *et al.*(*27*) showed from Mössbauer data that the Fe atom in $Fe_{1/4}VS_2$ is in a low-spin state. In contrast with this result, the Fe atom in $Fe_{1/4}TiS_2$ is in a high-spin state. This difference may arise from the difference in the magnetic properties of the host matrix: VS_2 has a magnetic moment but TiS_2 does not. From the Mössbauer data on $Fe_{1/4}TiS_2$ it may be concluded that the absence of magnetic ordering in $Fe_{1/4}VS_2$ is related to a host–matrix spin–spin interaction which is not present in the case of the titanium chalcogenide system.

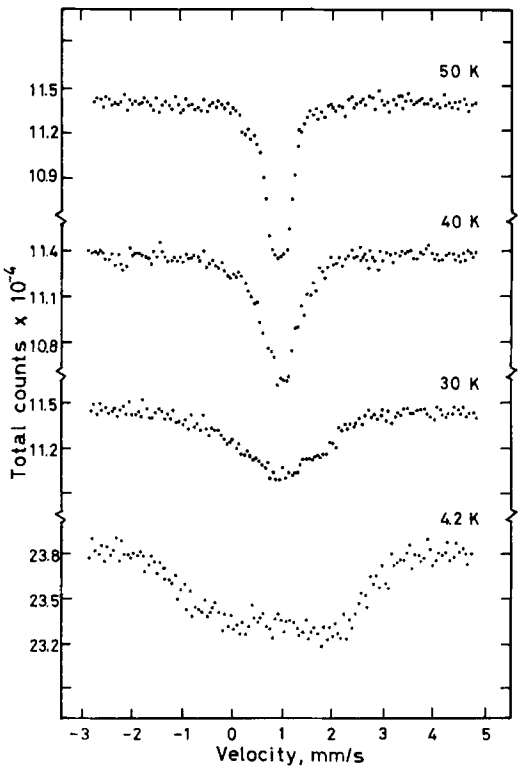

FIG. 3. Mössbauer spectra of $Fe_{1/4}TiS_2$ at four temperatures in the temperature range $4.2 \leq T \leq 50$ K.

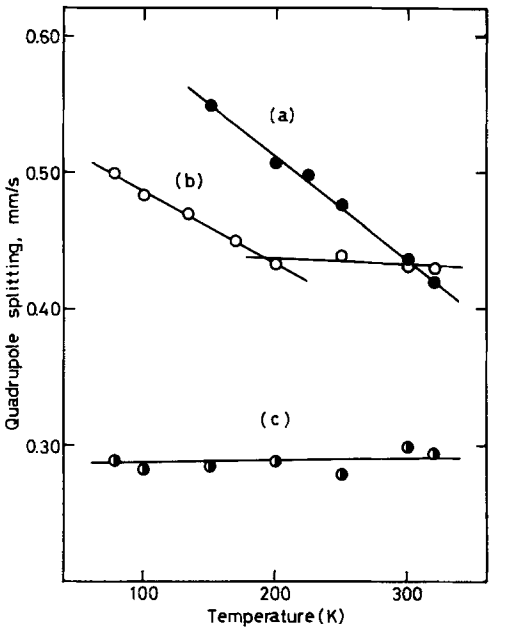

FIG. 4. Temperature dependence of the quadrupole splitting of the intercalation compounds in the temperature range $78 \leq T \leq 320$ K. (a) $Fe_{1/2}TiS_2$, (b) $Fe_{1/3}NbS_2$, and (c) $Fe_{1/4}TiS_2$.

Quadrupole Splitting

The temperature dependence of the quadrupole splitting parameter in $Fe_{1/2}TiS_2$, $Fe_{1/3}NbS_2$, and $Fe_{1/4}TiS_2$ is shown in Fig. 4.

In general, high-spin ferrous compounds have a large and temperature-dependent quadrupole splitting because the major contribution to the field gradient is due to an extra electron beyond the half-filled d^5 configuration which can distort the symmetry of the electronic environment of the Fe atom. The temperature dependence of the relative electron population in these d orbitals leads to a temperature-dependent quadrupole hyperfine interaction.

In the case of $Fe_{1/4}TiS_2$, the quadrupole hyperfine interaction is almost temperature

independent. This indicates that the relative population of electrons in the five *d* orbitals is not dependent on temperature; that is, the energy separation of the ground state orbitals is small compared to *kT*, even at the lowest temperatures at which the QS interaction can be accurately determined from the spectral data. On the other hand, the quadrupole splittings of $Fe_{1/2}TiS_2$ and $Fe_{1/3}NbS_2$ show an appreciable temperature dependence which may be related to the temperature dependence of the trigonal component of the crystalline field as well as that of the electron population, the thermal dependence of which is given by the Boltzmann distribution.

The quadrupole hyperfine interaction can be used as a criterion of the departure of the structure from cubic symmetry only if it can be assumed (or if one can estimate from other data) that the electronic component of the QS interaction is zero.[1] The values of the IS and QS parameters reported in Table I suggest very strongly that there is a significant delocalization of minority *p*-spin electrons, presumably arising from iron–iron or iron–chalcogen–iron bonding interactions. In this case, the quadrupole hyperfine interaction reflects the trigonal component of the crystalline field. Under these conditions the temperature dependence of the QS parameter reflects the anisotropic trigonal field, and in particular the thermal variation of the axial *c*/*a* ratio, rather than the temperature dependence of the electron populations. It has been suggested[1] that this is the situation which obtains in FeS, Fe_7S_8, and Fe_3S_4.

The discontinuous temperature dependence of the quadrupole splitting of $Fe_{1/3}NbS_2$ suggests that this compound has a second-order phase transition at about 200 K. This transition is due to a distortion of the octahedral environment around the iron atom in this compound, and is completely reversible as judged from the identity of the Mössbauer resonance parameters observed in a warming cycle as compared to a cooling cycle through the transition temperature. It is interesting to note that such a reversible transition was not observed in our previous work on the related compound $Sn_{1/3}NbS_2$ (*16*).

As can be seen in Table I, the values of the isomer shift and quadrupole splitting, respectively, for all of the subject compounds are very similar. This result may be accounted for by the essential constancy of the nearest neighboring environment of Fe atoms in these compounds as shown in Fig. 5, in which, for clarity, only the metal atoms are shown in the crystal structures. These geometries can be described as defect NiAs-type structures with part of the cation sites unoccupied. The titanium layer is completely occupied, while the iron layer is only partially filled, with the Fe atoms and vacancies forming an ordered arrangement. If the Fe atoms and vacancies were not ordered and/or the Fe and Ti atoms were not located in every second metallic layer, two or more distinct iron sites would exist. Mössbauer spectra of all the intercalates, however, showed only one iron site as judged from the linewidths observed well

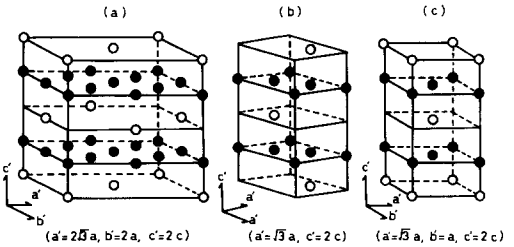

FIG. 5. Crystal structures of (a) $Fe_{1/4}TiS_2$, (b) $Fe_{1/3}TiS_2$ and $Fe_{1/3}NbS_2$, and (c) $Fe_{1/2}TiS_2$. The S atoms are not shown for clarity. $Fe_{1/4}TiS_2$ and $Fe_{1/2}TiS_2$ have a monoclinic supercell, whereas $Fe_{1/3}TiS_2$ and $Fe_{1/3}NbS_2$ have a trigonal supercell. Parameters *a* and *c* are the lattice parameters for the original TiS_2 and NbS_2 cells. ○, Fe; ●, Ti and Nb.

[1] The authors are indebted to one of the reviewers of this manuscript for commenting on this point in some detail.

above the magnetic ordering temperature. This result suggests that the metal atoms and the vacancies form ordered arrangements, with the iron atoms occupying a unique lattice position.

Temperature Dependence of the Recoil-Free Fraction

The isomer shift and quadrupole splitting Mössbauer parameters only yield information relating to the nearest-neighbor environments of the resonant atom, such as details of the chemical bonding and the spatial distribution of electrons, while the recoil-free fraction and its temperature dependence provide information about the lattice dynamical properties of the solid state which are associated with the motion of the Mössbauer atoms.

The temperature dependence of the recoil-free fraction for the ^{57}Fe Mössbauer transition can be extracted from the temperature dependence of the area under the resonance curve, and such data for the systems Fe_xTiS_2 and $Fe_{1/3}NbS_2$ are summarized in Fig. 6. The temperature dependence can be used to calculate a value of the Mössbauer lattice temperature, θ_M, from the relationship

$$\frac{d \ln f}{dT} = \frac{d \ln[A(T)/A(78)]}{dT} = \frac{-3E_\gamma^2}{Mc^2\kappa\theta_M^2}, \quad (1)$$

if the assumption is made that the effective vibrating mass, M, is the mass of a "bare" iron atom. In Eq. (1), E_γ is the Mössbauer γ-ray transition energy and κ is the Boltzmann constant. The area under the resonance curve at temperature T has been normalized to that at liquid nitrogen temperature, $A(78)$.

The effective vibrating mass, M, can be extracted from the temperature dependence of the isomer shift; that is,

$$\frac{d\mathrm{IS}}{dT} = \frac{-3E_\gamma\kappa}{2Mc^2}. \quad (2)$$

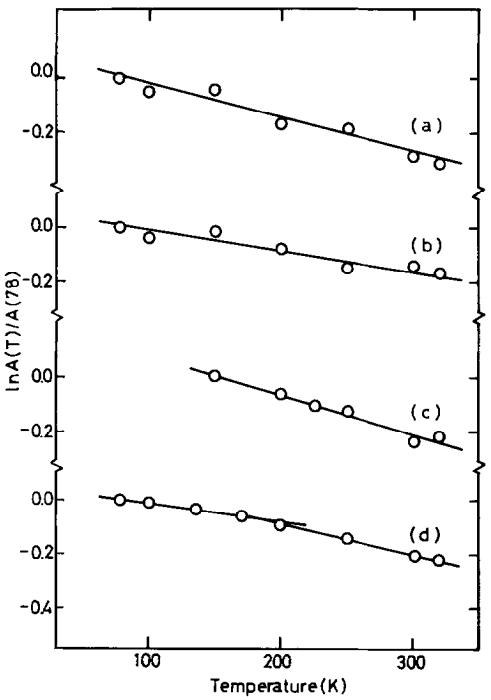

FIG. 6. Temperature dependence of the area under the resonance curve (normalized to the 78 K point except for $Fe_{1/2}TiS_2$ (150 K)) for (a) $Fe_{1/4}TiS_2$, (b) $Fe_{1/3}TiS_2$, (c) $Fe_{1/2}TiS_2$, and (d) $Fe_{1/3}NbS_2$. The straight line is a linear least-squares fit to the data over the pertinent temperature interval.

Combination of Eqs. (1) and (2) leads to the relationship

$$\theta'_M = \frac{(2E_\gamma)^{1/2}}{\kappa}\left[\frac{d\mathrm{IS}/dT}{d \ln[A(T)/A(78)]/dT}\right]^{1/2}, \quad (3)$$

which, in the case of ^{57}Fe, has the value

$$= 4.327 \times 10^2 \left[\frac{d\mathrm{IS}\, dT}{d \ln[A(T)/A(78)]/dT}\right]^{1/2}. \quad (3')$$

The values of the lattice temperature calculated using the $d\mathrm{IS}/dT$ and $d \ln A/dT$ data for Fe_xTiS_2 and $Fe_{1/3}NbS_2$ are summarized in Table II, together with the effective vibrating mass evaluated using Eq. (2). The similarity between the lattice temperatures θ_M and θ'_M implies that the vibrating mass in these compounds is close to that of a "bare" iron atom. This result may be ac-

TABLE II

SUMMARY OF MÖSSBAUER LATTICE TEMPERATURES FOR Fe_xTiS_2 ($x = \frac{1}{4}, \frac{1}{3}$, AND $\frac{1}{2}$) AND $Fe_{1/3}NbS$[a]

Absorber	θ_M (K)	θ'_M (K)	Effective mass (a.m.u.)	Temperature range (K)
$Fe_{1/4}TiS_2$	330 ± 5	316 ± 10	62 ± 6	78–320
$Fe_{1/3}TiS_2$	448 ± 5	415 ± 10	67 ± 6	78–320
$Fe_{1/2}TiS_2$	323 ± 5	323 ± 10	57 ± 6	150–320
	423 ± 5	381 ± 10	71 ± 6	78–200
$Fe_{1/3}NbS_2$	362 ± 5	344 ± 10	63 ± 6	200–320

[a] The larger error associated with the θ'_M parameter arises from the additional errors involved in the temperature dependence of the isomer shift, as compared to the θ_M values.

counted for as follows: It has been observed previously (*29*) that in many covalent solids made up of discrete molecular units held together by relatively weak intermolecular forces, the effective vibrating mass extracted from the Mössbauer data corresponds very closely to the molecular weight of the molecular unit. In the present instance, the three-dimensional metal–sulfur matrix is held together by strong interatomic bonding forces while the intercalant "guest" atom is held in the structure by much weaker forces. Under such conditions, although there is not a complete separability of the phonon spectrum of the matrix and of the "guest" atom, the latter may be expected to reflect the motion corresponding nearly to a single atom mass. Thus, in the absence of strong bonding forces between the matrix and the intercalant atom, the latter will evidence an effective vibrating mass which is very nearly that of a "bare" iron atom, in agreement with experimental observation that $\theta_M \approx \theta'_M$. Both of these parameters will be characteristic of the particular matrix in which the intercalant atom is held. In this context it is interesting to note that despite the similarity in the nearest-neighbor environments about the iron atom in these structures, the lattice temperatures, θ_M, are quite different for the different matrices, indicating that the dynamical properties of the iron atoms in these lattices are not identical. The highest lattice temperature observed is that for $Fe_{1/3}TiS_2$ which is assumed to be isostructural with $Fe_{1/3}NbS_2$. The differences in the lattice temperatures arise presumably through differences in the sulfur–metal atom bridging bonds in the several structures.

As shown in Fig. 7, there are three kinds of sulfur atoms in these structures which must be considered. In this representation, only one side of the sulfur layers and the iron atom are shown. S_I (solid circle) has an environment of three Ti atoms, two Fe atoms, and one vacancy. S_{II} (half-solid circle) has an environment of three Ti atoms, one Fe atom, and two vacancies, while S_{III} (open circle) has an environment of three Ti atoms and three vacancy sites. This kind of sulfur atom (S_{III}) is not directly involved in

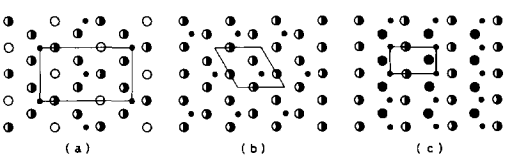

FIG. 7. Idealized arrangement of Fe and S atoms in (a) $Fe_{1/4}TiS_2$, (b) $Fe_{1/3}TiS_2$ and $Fe_{1/3}NbS_2$, and (c) $Fe_{1/2}TiS_2$ viewed along the c axis (Fe atoms at $z = 0$; S atoms at $z = -\frac{1}{8}$). The solid line indicates a supercell. •, Fe; ●, S_I; ◑, S_{II}; ○, S_{III}.

bonding to the intercalant atom, but does contribute to the total bonding forces in the matrix. In the $Fe_{1/3}TiS_2$ structure, all of the sulfur atoms are of the same kind (S_{II}) while in $Fe_{1/4}TiS_2$ and $Fe_{1/2}TiS_2$ the lattice involves the different types of sulfur atoms discussed above. The higher lattice temperature observed in $Fe_{1/3}TiS_2$ (and presumably that for the isostructural $Fe_{1/3}NbS_2$, although the comparison data are not available) suggests that the Fe–S bridge bonds involving only S_{II} atoms give rise to a more rigid structure than that which obtains when S_I and/or S_{III} atoms are present in the matrix holding the iron atom. It should be emphasized that this conclusion is based on purely phenomenological arguments; that is, the relative values of θ_M (and θ'_M) for the several compounds discussed. Indeed it is not clear at this stage why the Mössbauer data for the iron atom in $Fe_{1/3}TiS_2$ reflect a more tightly bound structure than that in, for example, $Fe_{1/2}TiS_2$, given the larger number of vacancies in the former than in the latter. Additional data on the relationships between the Mössbauer lattice temperature and the microscopic details of the structure of intercalation compounds will be needed to elucidate this interesting point.

Acknowledgments

This research was supported in part by the National Science Foundation under Grants DMR-76-00139 and DMR-78-08615 as well as a grant from the Rutgers Center for Computer and Information Services for computational services. This support is herewith gratefully acknowledged. The authors are also indebted to Professor H. Kondo and Dr. T. Okada for numerous helpful discussions.

References

1. J. M. VAN DEN BERG AND P. COSSEE, *Inorg. Chim. Acta* **2,** 143 (1968).
2. F. HULLIGER AND E. POBITSCHKA, *J. Solid State Chem.* **1,** 117 (1970).
3. J. M. VOORKOEVE AND M. ROBBINS, *J. Solid State Chem.* **1,** 134 (1970).
4. K. ANZENHOFER, J. M. VAN DEN BERG, P. COSSEE, AND J. N. HELLE, *J. Phys. Chem. Solids* **31,** 1057 (1970).
5. B. VAN LAAR, H. M. RIETVELD, AND D. J. IJID, *J. Solid State Chem.* **3,** 154 (1971).
6. M. EIBSCHÜTZ, F. J. DISALVO, G. W. HULL, JR., AND S. MAHAJAN, *Appl. Phys. Lett.* **28,** 464 (1975).
7. R. H. FRIEND, A. R. BEAL, AND A. D. YOFFE, *Phil. Mag.* **35,**1269 (1977).
8. T. TAKAHASHI AND O. YAMADA, *J. Solid State Chem.* **7,** 25 (1973).
9. M. DANOT, J. ROUXEL, AND O. GOROCHEV, *Mater. Res. Bull.* **9,** 1383 (1974).
10. R. H. PLOVNIK, M. VLASSE, AND A. WOLD, *Inorg. Chem.* **7,** 127 (1968).
11. R. H. PLOVNIK, D. S. PERLOFF, M. VLASSE, AND A. WOLD, *J. Phys. Chem. Solids* **29,** 1935 (1968).
12. B. L. MORRIS, V. JOHNSON, R. H. PLOVNIK, AND A. WOLD, *J. Appl. Phys.* **40,** 1299 (1969).
13. S. MURANAKA, *Mater. Res. Bull.* **8,** 679 (1973).
14. S. MURANAKA AND T. TAKADA, *J. Solid State Chem.* **14,** 291 (1975).
15. K. OHASHI AND I. TSUJIKAWA, *J. Phys. Soc. Japan* **37,** 63 (1974), and references therein.
16. R. H. HERBER AND R. F. DAVIS, *J. Chem. Phys.* **63,** 3668 (1975); **65,** 3773 (1976).
17. J. G. BALLARD AND T. BIRCHALL, *J. Chem. Soc. Dalton,* 1860 (1976).
18. L. E. CAMPBELL, G. L. MONTET, AND G. L. PERLOW, *Phys. Rev. B* **15,** 3318 (1977).
19. M. KATADA AND R. H. HERBER, *J. Inorg. Nucl. Chem.* **41,** 1097 (1979), and references therein.
20. G. A. FATSEAS, J. L. DORMANN, AND M. DANOT, *J. Phys.* **37,** C6-579 (1976); **40,** C2-367 (1979).
21. F. K. LOTGERING AND R. P. VAN STAPELE, *J. Appl. Phys.* **39,** 417 (1968).
22. A. J. REIN AND R. H. HERBER, *J. Chem. Phys.* **63,** 1021 (1975), and references therein.
23. S. HAFNER AND M. KALVIUS, *Z. Kristallogr.* **123,** 443 (1966).
24. M. EIBSCHÜTZ, E. HERMON, AND S. SHTRIKMAN, *J. Phys. Chem. Solids* **28,** 1633 (1967).
25. R. H. HERBER AND M. KATADA, *J. Solid State Chem.* **27,** 137 (1979).
26. A. R. BEAL AND W. Y. LIANG, *Phil. Mag.* **33,** 121 (1976).
27. Y. OKA, K. KOSUGE, AND S. KACHI, *Mater. Res. Bull.* **12,** 1117 (1977).
28. S. R. HONG AND H. H. OK, *Phys. Rev. B* **11,** 4176 (1975).
29. R. H. HERBER, M. F. LEAHY, AND Y. HAZONY, *J. Chem. Phys.* **60,** 5070 (1974); A. J. REIN AND R. H. HERBER, *J. Chem. Phys.* **63,** 1021 (1975); R. H. HERBER AND M. F. LEAHY, *J. Chem. Phys.* **67,** 2718 (1977), and references therein.